GENERAL SYMPOSIA | POLYMER FOAMS AND MEMBRANES

From Vibrating Molecules to a Running Shoe: Connecting Dielectric Properties with Process Feedback in Radio-Frequency welding of TPU Bead Foams

Marcel Dippold, Makrina A. Chairopoulou, Maximilian Drexler, Michael Scheiber and Holger Ruckdäschel

DOI: https://doi.org/10.51573/Andes.PPS39.GS.PFM.1

December 2024

From Vibrating Molecules to a Running Shoe: Connecting Dielectric Properties with Process Feedback in Radio-Frequency welding of TPU Bead Foams

Marcel Dippold, Makrina A. Chairopoulou, Maximilian Drexler, Michael Scheiber and Holger Ruckdäschel[1]

Abstract: Besides new material solutions, innovative processing technologies are key for working towards a more sustainable future for bead foam products. Compared to standard steam chest molding, innovative radio frequency (RF) welding shows great potential based on its direct energy input, which results in reduced energy consumption. Thus, the present study provides fundamental insights into the correlation of dielectric properties of expanded thermoplastic polyurethane (ETPU) bead foams with the processing behavior. Impedance spectroscopy is used to analyze the complex relative permittivity ε_r^* of both polymer and respective beads. The dielectric properties of polymers are dictated by their molecular structure and hence resulting dipoles. Thus, significant dependency on temperature and frequency is observed due to changes in chain flexibility and therefore alignment with the oscillating electromagnetic field. As cellular structures, the introduction of a second air phase leads to generally attenuated values at equal trends. Within the RF process, changes, predominantly in the imaginary part of ε_r^* from initial starting temperatures up to welding, are directly reflected in the power curve as process feedback. Furthermore, temperature evolution and derived heating rate within the bead foams demonstrate excellent conformity with previous results with minor deviations due to the thermal inertia of the fiber optic temperature sensor.

Keywords: Radio Frequency, Bead Foams, Dielectric Properties, ETPU, Welding

1 Marcel Dippold, Michael Scheiber and Holger Ruckdäschel (holger.ruckdaeschel@uni-bayreuth.de) are affiliated with the University of Bayreuth in Germany. Makrina A. Chairopoulou and Maximilian Drexler are affiliated with Adidas AG in Germany.

DOI: https://doi.org/10.51573/Andes.PPS39.GS.PFM.1

Introduction

From packaging to sports equipment, bead foam products are integral to our daily lives. In recent decades, the market and research landscapes have seen the emergence of numerous new materials based on bio-based or recycled polymers [1]. Additionally, there has been a significant focus on developing technical and high-performance materials to expand their application range to higher operating temperatures. Alongside advancements in materials, new processing technologies have been introduced. These include the welding together of individual beads to create three-dimensional, durable parts in a more energy and resource efficient manner [2]. Among these innovations, the most notable is the direct dielectric heating of beads using an external electromagnetic field in the radio-frequency range [3]. This method generates heat through intermolecular friction within the polymer volume itself as dipoles within the affected volume interact with the oscillating field and undergo constant realignment [4-6]. A thorough investigation of these physical phenomena is essential to optimize the process for maximum energy efficiency and part quality. As shown in previous studies, the dielectric properties of these materials are key in order to understand and predict their interaction within the electromagnetic field and consequently their heating behavior [7]. In terms of values, the complex relative permittivity ε_r^* is a material property, influenced both by temperature and frequency [8]. Due to this superposition, changes over the length of the welding cycle starting with beads at room temperature up to the welding temperature are essential for fundamental process knowledge [7, 9, 10]. The direct link between permittivity and heating behavior is established by the volumetric power input P_v in Equation (1). [5,11].

$$P_V = 2 \times \pi \times f \times \varepsilon_0 \times \varepsilon_r'' \times E_{RMS}^2 \qquad 1)$$

ε_0 represents the permittivity of vacuum and f the frequency of the oscillating electromagnetic field with E_{RMS} as the root mean square (RMS) value of the peak field strength. The imaginary part ε_r'' of the complex-valued relative permittivity ε_r^* is therefore in linear dependency to the intrinsic heating power of any material within an oscillating electromagnetic field. Despite no visible correlation to the real part of the relative permittivity ε_r' within the shown Equation (1), an indirect impact is known via the electromagnetic field strength E_{RMS}. This interaction is based on the influence of this material property on the capacity within a serial stack as well as the field displacement between phases with different permittivity [12]. For the intricate multi-phase system of RF bead foam welding, both phenomena may occur. However, their magnitude is difficult to estimate without complex simulative approaches. Thus, the present study first analyzes the permittivity of both bulk polymer and bead foams in order to subsequently link these material properties with the direct process feedback during the RF welding.

Materials and Methods

Materials

Within this study, the commercially available ETPU grade Infinergy® 32-100 U10 from BASF SE (Ludwigshafen, Germany) was used with an average bead density of 183 kg/m³. For the analysis of the bulk polymer properties, hot pressing was utilized to compact the beads and produce solid platelets with a diameter of 25 mm and a height of 1 mm.

Impedance Spectroscopy

The permittivity of the material was measured with RF I-V method by the E4991A RF impedance analyzer from Keysight Technologies, Inc. (Santa Rose, USA) and an UF55plus universal oven by Memmert GmbH + Co. KG (Schwabach, Germany). The bulk material and bead foams at defined densities were analyzed within two specially designed measurement cells. A detailed explanation of the setup can be found in a previous study [7].

Radio Frequency Welding

The radio frequency welding trials were conducted on a Wave Foamer C from Kurtz GmbH & Co. KG (Kreuzwertheim, Germany). A schematic representation of the setup with active and ground electrodes, PTFE mold, and filled beads is illustrated in Figure 1(a).

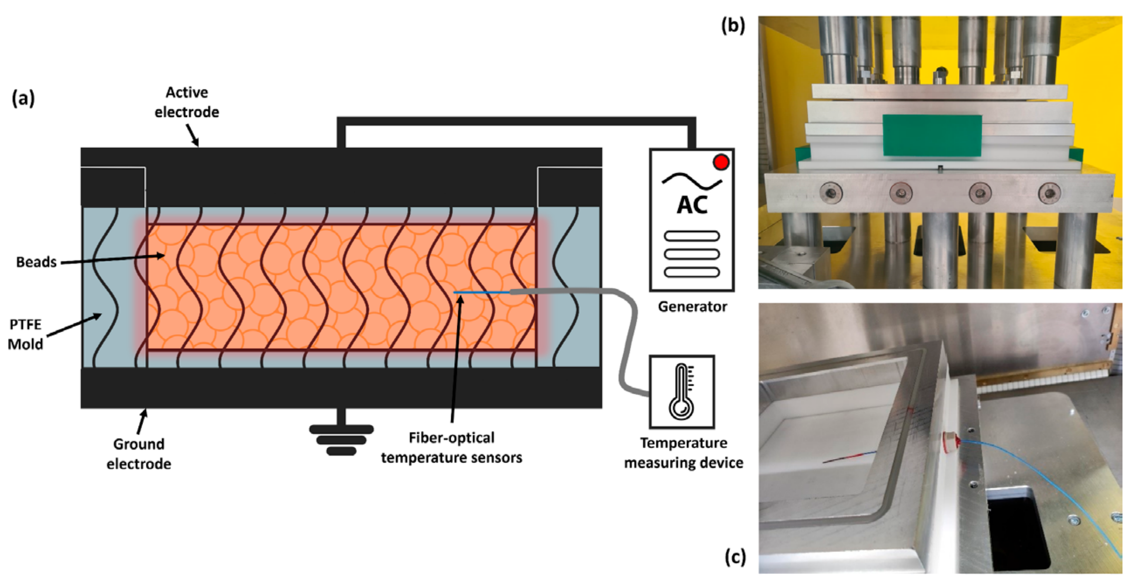

Figure 1. Schematic cross-section of the mold with beads and temperature sensor (a), real PTFE mold with upper and lower electrode installed in the RF machine (b), and detailed view of the temperature sensor entering the empty mold (c).

The alternating current generator is connected to the upper active electrode, setting the potential difference to the lower ground electrode, thus resulting in an oscillating electromagnetic field with a fixed frequency of 27.12 MHz. The maximum voltage for all trials was set to 9 kV with a short ramp-up time of around 4 s. Durations at this maximum voltage varied between 12.5 and 25 s. The density of the plates was controlled by weight and set to a fixed 25 vol.-% of polymer with respect to the mold volume. This results in a part density of 276 kg/m³. Before demolding, a stabilization time of 200 s was set in order to ensure sufficient cooling. A PTFE frame with an internal rectangular geometry of 200 x 200 mm² was used as a mold (Figure 1[b]). PTFE isolation plates below and above the foam beads set the height of the final foam sample to 10 mm. Since conductive materials would strongly interact with the electromagnetic field, a special fiber optic temperature sensor was placed within the bead foam to measure its temperature increase. As shown in Figure 1(c), the cable is fed through a sealed entry port on the right side of the frame. To ensure representative results, a central positioning of the sensor within the plate was analyzed after each trial throughout the cross-section.

Results and Discussion

Dielectric Properties of ETPU

The permittivity of polymers and their dependency on temperature and frequency is based on their chemical structure and resulting molecular interactions across individual chains. As shown in literature, ε_r' exhibits a step down behavior over frequency [7]. Due to internal relaxation processes, this phenomena is also visible for the investigated TPU in Figure 2.

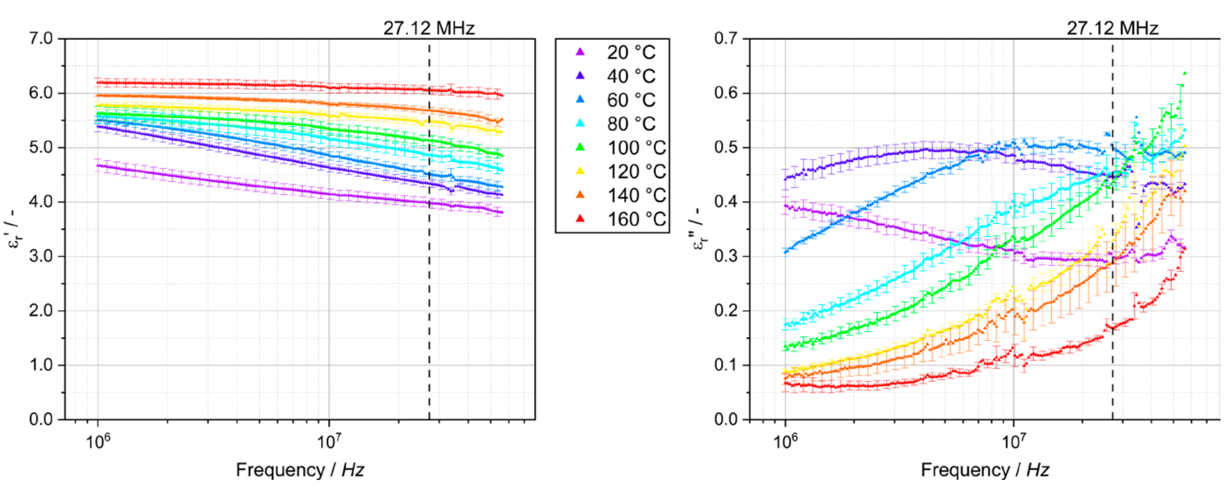

Figure 2. Real and imaginary parts of the complex relative permittivity ε_r^* of TPU as a function of frequency from 20 to 160°C.

Enhanced flexibility of the polymer chains at elevated temperatures resulting in a shift of that step to higher frequencies resulted in increased permittivity values at a constant frequency. Since the analysis frequency range is limited by the setup from 1 to 50 MHz, the step down is only partially visible at each temperature. A similar behavior is observed for ε_r''. Here, a peak is formed over frequency, which constantly shifts upwards if the temperature is increased. The peak of ε_r'' corresponds to the inverse relaxation time of the orientational polarization phenomena within the chain's dipoles. Elevated flexibility allows the dipoles to align up to faster alternating fields and therefore lower their specific relaxation time. At temperatures above 60°C, the tip of the peak is out of the observable frequency range and only the left shoulder of the peak is visible.

Since the frequency of the electromagnetic field within the RF process is fixed at 27.12 MHz for regulatory reasons, the real and imaginary part over the temperature at individual frequencies are shown in Figure 3.

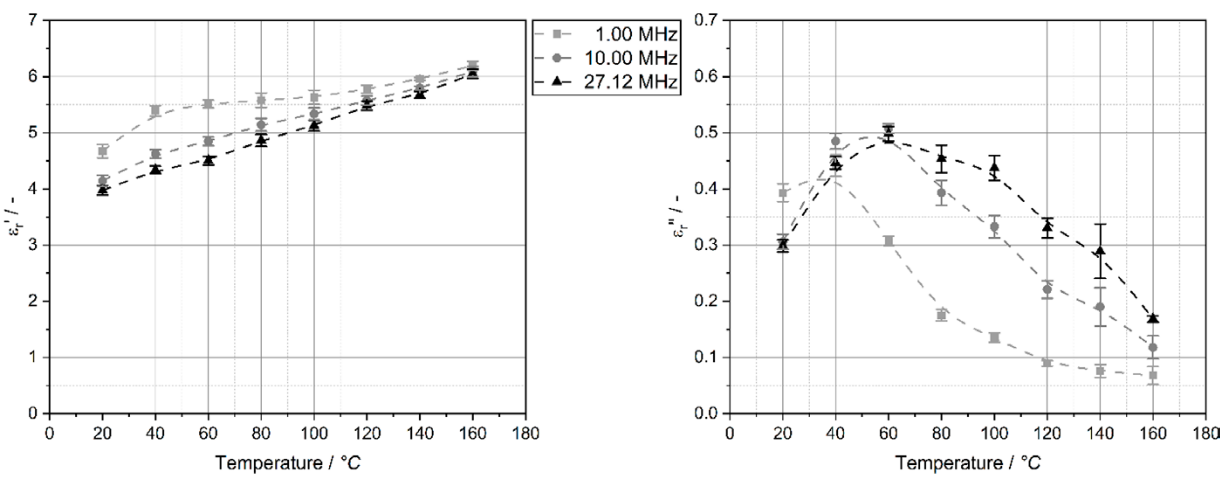

Figure 3. Real and imaginary part of the complex relative permittivity ε_r^* of TPU as a function of temperature at frequencies of 1, 10, and 27.12 MHz.

The previously mentioned superposition of temperature and frequency is clearly observable in ε_r'. Over the temperature, this behavior results in a step up towards higher temperatures, visible for 1 MHz. At higher frequencies of 10 and 27.12 MHz, this feature is less distinctive, and a more gradual incline can be observed. This material response is based on a combination of relaxation phenomena and an overall increased chain flexibility with increasing temperature, thus leading to reduced intermolecular interactions [13, 14]. Similar to ε_r', the ε_r'' peak exhibits a shift to elevated temperatures with an increase in analysis frequency. At the fixed frequency of 27.12 MHz, changes in the real but primarily imaginary part of the complex relative permittivity over the welding period must be considered. These changes will directly impact the heating of the material based on the volumetric power input from Equation (1).

DOI: https://doi.org/10.51573/Andes.PPS39.GS.PFM.1

In addition to the bulk TPU material, a second bigger measurement cell allows for direct analysis of the complex relative permittivity of the beads at defined densities and temperatures [7]. Dielectric properties of multi-phase systems are subject to complex interactions within and between the individual materials. This causes them to deviate from a simple linear mixing rule [15-17]. Figure 4 shows a similar behavior in ε_r' and ε_r'' of the beads at a density of 15 vol.-% of the polymer at all temperatures compared to the prior bulk TPU.

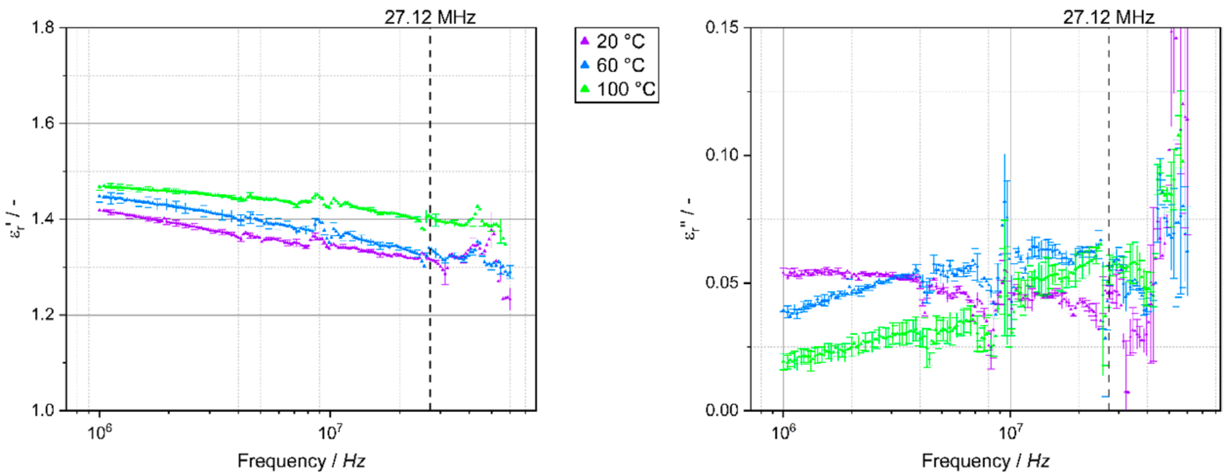

Figure 4. Real and imaginary part of the complex relative permittivity ε_r^* of ETPU as a function of frequency at a defined density of 15 vol.-% at 20, 60 and 100°C.

Despite showing a similar overall trend over the frequency, the quantity of both parts of the complex relative permittivity is attenuated since the second phase air has generally lower values ($\varepsilon_r^* = 1 - 0i$). Thus, the average response of the material within the measurement cell is reduced. This results in increased deviations, which is especially visible in ε_r'' at higher frequencies limited by internal resonances.

At a fixed temperature, the ratio of polymer within the analyzed volume of beads is the determining parameter, as shown in Figure 5. As expected, the values for ε_r' and ε_r'' are in between the two polymer and air phases, depending on the volumetric ratio with again similar trends to the bulk TPU. During the production of parts with increased density, this will automatically lead to elevated power input. However, a higher amount of polymer will also increase the volumetric heat capacity of the system linearly with density. This leads to theoretically similar heating rates independent of the density for a fixed material. Nevertheless, this only represents a highly simplified assumption. Elements like local displacement of the electromagnetic field within the cellular structure and to the mold is excluded as well as thermal conductivity within the bead foam and towards the PTFE frame and isolation plates.

DOI: https://doi.org/10.51573/Andes.PPS39.GS.PFM.1

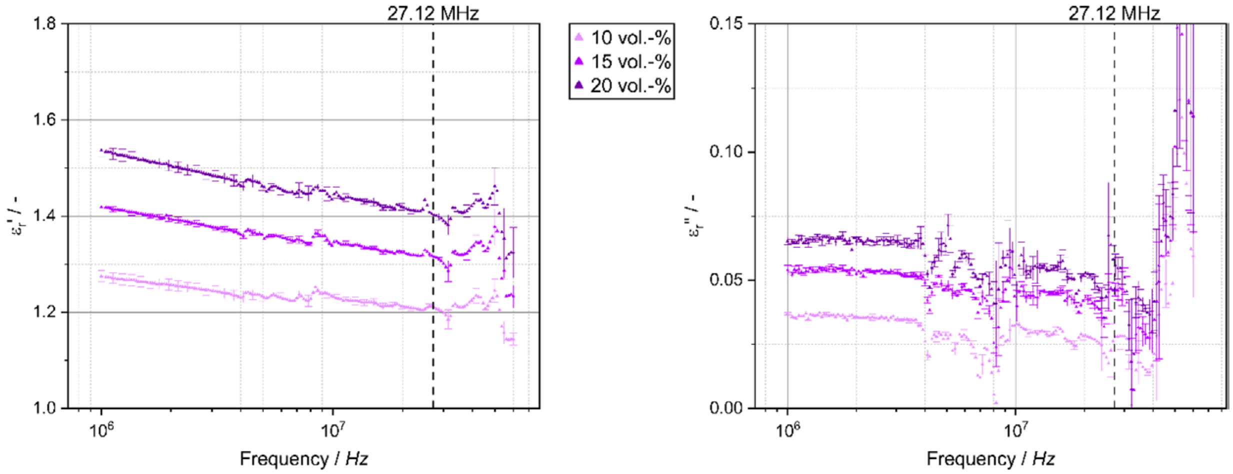

Figure 5. Real and imaginary part of the complex relative permittivity ε_r^* of ETPU as a function of frequency at 20°C and defined densities of 10, 15 and 20 vol.-%.

Influence of Dielectric Properties on Radio Frequency Welding

In order to verify the connection between material properties and the RF process, multiple welding trials were conducted. The real voltage present at the active electrode is shown in Figure 6.

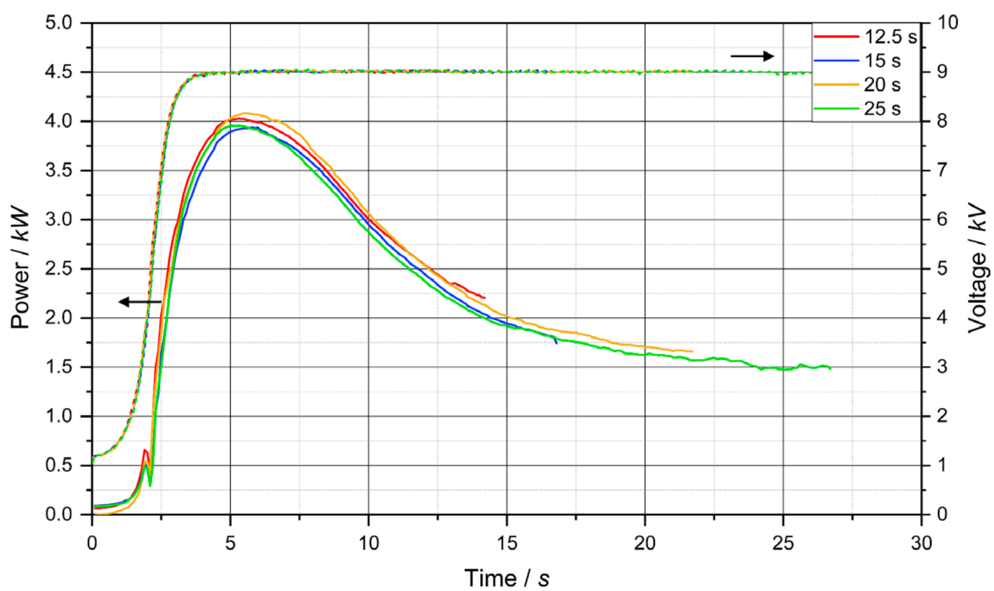

Figure 6. Power and voltage as a function of time for the welding trials at 9 kV with 25 vol.-% of beads for times at maximum voltage at 12.5, 15, 20, and 25 s.

The voltage curve over time is predetermined by the operator with a linear ramp-up at the beginning of 2 s until the maximum voltage of 9 kV is reached. Due to machine-related inertia within the voltage regulation, the initial phase deviates from that specification. This results in a slight delay in the ramp-up. A constant voltage is reached after approximately 4 s. Neglecting the only slight changes in ε_r', a fixed voltage results in a constant electromagnetic field strength. Based on the plate geometry it can be assumed to be homogeneous with only minor edge effects. Thus, the observable changes in power over the welding time may be attributed to evolving ε_r'' with increased temperature. As expected, all curves with changing time at maximum voltage from 12.5 to 25 s are overlapping. This indicates a high reproducibility of the process and feedback data. Within the range of constant voltage, an initial slight increase in power up to a maximum is followed by an elongated decline. By comparing the results of ε_r'' (Figure 3) with this behavior, the linear dependency between this material property and the process feedback is clearly visible. With the peak power at around 5 to 6 s a temperature of around 60°C can be reversely attributed.

This indirect temperature observation can be compared to the data of the fiber optic temperature sensor placed inside the beads during the welding process (Figure 7).

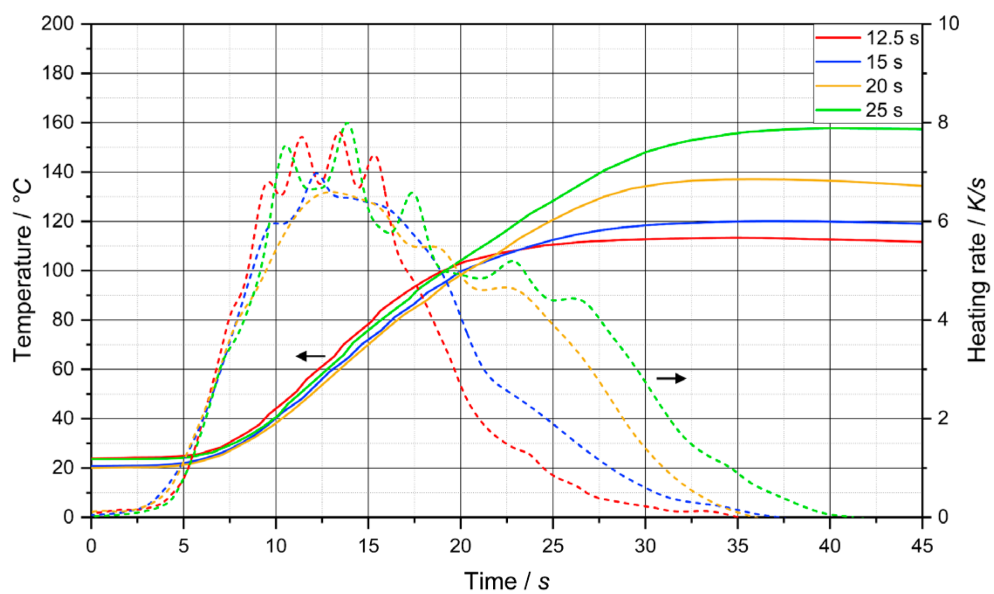

Figure 7. Temperature and calculated heating rate as a function of time for the welding trials at 9 kV with 25 vol.-% of beads for times at maximum voltage at 12.5, 15, 20, and 25 s.

A significant delay is clearly visible in the expected temperature to the measured one. Despite the small diameter of the 1 mm sensor tip, the apparent thermal inertia must be considered when interpreting the data. Furthermore, this phenomenon is reflected in the initial delay of around 5 s until the temperature starts to rise. Additionally, a continuous temperature increase is observed exceeding the time frame of applied voltage by up to 15 s. This also suggests that the maximum

DOI: https://doi.org/10.51573/Andes.PPS39.GS.PFM.1

temperatures measured during the process underestimate the actual ones with a high probability. Temperature is by far the most important parameter for the welding of the individual beads to a final part. This deviation must therefore be considered in understanding and optimizing the process in combination with the respective material. Additionally, the heating rate can be calculated from the temperature curve over time. At a constant heat capacity, the heating rate is directly proportional to the volumetric power input by the dielectric heating of the polymer. After an initial peak in heating rate a slight drop is observable for all welding times. Once the voltage is switched off, the thermal inertia still leads to positive heating rates, but with decreasing strength until cooling occurs. Thus, by comparing all individual results, a direct correlation between the temperature-dependent dielectric properties of the polymer and both feedback curves power and heating rate at the RF process is visible.

Conclusion

This study provides a clear correlation between the material properties and process feedback during the novel RF welding process. The permittivity of the TPU as bulk material shows significant changes throughout the analyzed frequency and temperature range. For ε_r', a step down is visible towards higher frequency with an overall increase for elevated temperature. Within the imaginary part ε_r'', however, a peak is formed that similarly shifts towards higher frequency at increased temperature. Focusing on fixed frequencies, as in the case of the RF process at 27.12 MHz, this leads to an initial rise in ε_r'' followed by a slow decline towards temperatures close to melting of the polymer. Switching to bead foams, the inclusion of a second air phase with constant properties when heated results in overall similar curves in permittivity, but with attenuated values in between the two individual materials. The power consumption within the RF process is directly correlated to material and process parameters. This behavior is clearly visible at a constant voltage after the initial ramp-up time. Here the temperature-induced changes in power over the welding time can be attributed to an evolving imaginary part of the relative permittivity ε_r''. Observations gained by the fiber optic temperature sensor are again mainly consistent with these theoretical correlations. Only a significant delay due to thermal inertia of the sensor was monitored. This indicates that an indirect analysis of the temperature via power appears to provide feedback without time delay. Thus, the insights gained within this study into the novel RF process for ETPU bead foams expand to new possibilities for a more sustainable future for lightweight products.

Acknowledgments

The authors would like to acknowledge Marc Norridge and Korbinian Berner for supporting the trials at the RF welding machine. Additionally, the Bavarian Polymer Institute (BPI) must be acknowledged for providing access to different analytical methods.

DOI: https://doi.org/10.51573/Andes.PPS39.GS.PFM.1

This research was funded by the “Bavarian Ministry of Economic Affairs, Regional Development and Energy” within the funding program “Verbundforschungsprogramm Förderlinie Materialien und Werkstoffe” (grant number MW-2104-0005).

References

1. D. Raps, N. Hossieny, C. B. Park, and V. Altstädt, “Past and present developments in polymer bead foams and bead foaming technology,” *Polymer (Guildf).*, vol. 56, pp. 5–19, 2015, https://doi.org/10.1016/j.polymer.2014.10.078
2. J. Kuhnigk, T. Standau, D. Dörr, C. Brütting, V. Altstädt, and H. Ruckdäschel, “Progress in the development of bead foams – A review,” *Journal of Cellular Plastics*, vol. 58, no. 4, pp. 707–735, 2022, https://doi.org/10.1177/0021955X221087603
3. V. Romanov, “Device and method for producing a particle foam part,” WO 2017/125412 A1, 2017.
4. N. Hossieny, M. Nofar, V. Shaayegan, and C. B. Park, “Effects of glycerol monosterate on TPUs crystallization and its foaming behavior,” *AIP Conference Proceedings*, vol. 1593, pp. 374–377, 2014, https://doi.org/10.1063/1.4873803
5. M. Mehdizadeh, *Microwave/RF Applicators and Probes for Material Heating, Sensing, and Plasma Generation: Second Edition*. 2015.
6. Zhou Y.; Breyen M, *Joining and assembly of medical materials and devices*. Woodhead Publishing Limited, 2013.
7. M. Dippold, C. Töpfer, and H. Ruckdäschel, “Influence of dielectric properties of polybutylene terephthalate and respective foam beads on process behavior in radio-frequency welding,” *Journal of Applied Polymer Science*, vol. 141, no. 8, pp. 1–12, Feb. 2024, https://doi.org/10.1002/app.54988
8. A. K. Jonscher, “A new model of dielectric loss in polymers,” *Colloid and Polymer Science*, vol. 253, no. 3, pp. 231–250, 1975, https://doi.org/10.1007/BF01470233
9. D. C. Campos, “Dielectric properties of polyols, at frequency range 0.2–3 GHz and temperature range 293–473 K: an analysis in the frequency and temperature domain,” *Journal of Microwave Power and Electromagnetic Energy*, vol. 54, no. 2, pp. 125–160, 2020, https://doi.org/10.1080/08327823.2020.1755482
10. T. Sabu, T. Raju, K. Z. Ajesh, and K. M. Raghvendra, *Spectroscopy methods for nanomaterials characterization*, vol. 2. Amsterdam: Elsevier Inc., 2017.
11. H. Sussner, D. E. Horne, and D. Y. Yoon, “A new method for determining the pyroelectric coefficient of thin polymer films using dielectric heating,” *Applied Physics Letters*, vol. 32, no. 3, pp. 137–139, 1978, https://doi.org/10.1063/1.89974
12. K. Schneider, C. Ott, and D. Drummer, “Simulative study of polymeric core–shell foam particles for the enlargement of the material portfolio in 3-D high-frequency welding ,” *Polymer Engineering & Science*, November, pp. 1–11, 2021, https://doi.org/10.1002/pen.25861

13. C. B. Roth and J. R. Dutcher, "Glass transition and chain mobility in thin polymer films," *Journal of Electroanalytical Chemistry*, vol. 584, no. 1, pp. 13–22, 2005, https://doi.org/10.1016/j.jelechem.2004.03.003

14. V. A. Bershtein, M. Z. Petkevich, L. G. Razgulyayeva, and V. A. Stepanov, "The temperature dependence of intermolecular interaction in polymers in the glassy state," *Polymer Science U.S.S.R.*, vol. 20, no. 12, pp. 3005–3013, 1978, https://doi.org/10.1016/0032-3950(78)90514-2

15. A. H. Sihvola, "How strict are theoretical bounds for dielectric properties of mixtures?," *IEEE Transactions on Geoscience and Remote Sensing*, vol. 40, no. 4, pp. 880–886, 2002, https://doi.org/10.1109/TGRS.2002.1006369

16. H. Looyenga, "Dielectric constants of heterogeneous mixtures," *Physica*, vol. 31, no. 3, pp. 401–406, 1965, https://doi.org/10.1016/0031-8914(65)90045-5

17. A. H. Sihvola and J. A. Kong, "Effective permittivity of dielectric mixtures," *IEEE Transactions on Geoscience and Remote Sensing*, vol. 26.4, pp. 420–429, 1988.

DOI: https://doi.org/10.51573/Andes.PPS39.GS.PFM.1